

Yi Min Wei · Tomoyuki Fujii · Yasushi Hiramatsu
Atsushi Miyatake · Shuichiro Yoshinaga · Tsuyoshi Fujii
Bunichiro Tomita

A preliminary investigation on microstructural characteristics of interfacial zone between cement and exploded wood fiber strand by using SEM-EDS

Received: April 18, 2003 / Accepted: July 17, 2003

Abstract The hydration behavior and strength performance of cement mixed with exploded wood fiber strand (WFS) obtained by the water-vapor explosion process have been studied previously. In the current study, the microstructural characteristics of cement–exploded WFS interfacial zone were examined using scanning electron microscopy with energy-dispersive X-ray spectroscopy (SEM-EDS). The Ca/Si ratios at the interfacial zones and the elemental compositions of hydration products deposited in the tracheid lumen were investigated. In addition, the morphological differences and compositional variations of hydration products that developed on the wood surfaces were examined. The results revealed that the Ca/Si ratios at the interfacial zones were strongly influenced by the mixture compositions, and that the elemental compositions of the hydration products that filled the tracheid lumen were significantly different from those of the cement paste in the mixtures. Differences in morphology and composition of hydration products at the wood surfaces were also observed to correspond to the different mixture compositions. These characteristics are considered to be directly related to the bond property, and thus, to the mechanical performance of WCM.

Key words Wood–cement mixture · Interfacial zone · Cement hydration · Inhibitory · SEM-EDS

Y. Wei (✉) · B. Tomita
Institute of Agricultural and Forest Engineering, University of
Tsukuba, Tsukuba 305-8572, Japan
Tel. +81-29-853-4578; Fax +81-29-855-2203
e-mail: s995176@icho.ipe.tsukuba.ac.jp

T. Fujii · Y. Hiramatsu · A. Miyatake · S. Yoshinaga · T. Fujii
Forestry and Forest Products Research Institute (FFPRI), Tsukuba
305-8687, Japan

Part of this report was presented at the 53rd Annual Meeting of the Japan Wood Research Society, Fukuoka, March 2003

Introduction

Wood–cement mixture (WCM) can be, as is well known, commercially used with its high acceptance for building purposes, because it possesses many advantages, which include water, fire, decay, moisture, and weather resistance, low cost, and simple production processes, over conventional wood-based building materials. However, many previous studies have pointed out that wood materials do not always react favorably with cement. The nature and quantity of wood components such as its water- or alkali-extractives, which are significantly different according to wood species or the treatment methods and conditions of the wood, critically affect the cement hydration, thereby inhibiting or entirely obstructing the formation of cement hydration products essential for strength development of WCM. The complex chemical and physical interactions caused by the some wood components, sometimes known as “cement poison,” that significantly influence the bond property between wood and cement are poorly understood at present.^{1–5}

In consideration of the increasing environmental concerns about the disposal of wood wastes (forest waste and construction waste), a patent technology known as the water-vapor explosion process (WVEP) was developed at the Forestry and Forest Products Research Institute (FFPRI) as a new method for the recycling of wood wastes. By this treatment process, a wide variety of wood wastes can be rapidly defibered into exploded wood fiber strand (WFS), which has potential for further application.^{6,7}

In order to explore the possibility of using exploded WFS as a potential raw material for WCM production, previous investigations have been mainly focused on obtaining a comprehensive understanding of the essential hydration behavior of exploded WFS–cement mixture, and the improvement in its compatibility and strength performance. Prior assessments gave an affirmative answer that exploded WFS could be used as an acceptable wood reinforcement material in WCM by means of addition with suitable additive chemicals and contents, even though the excessive

water-soluble and low molecular weight degraded polysaccharides were found in its extractives.^{8,9}

Many factors are associated with the mechanical performance of WCM. However, the nature and properties of the wood–cement interfacial zone are thought to be of primary significance and play an important role, even in the overall behavior of WCM. A strong bond between wood and cement provides WCM with strength, whereas a weak bond results in WCM lacking strength. In fact, the improvement in mechanical performance of WCM is also largely attributed to the enhancement of bond strength between wood and cement. In addition, WCM is significantly different from the reinforcement materials that are usually used in cement or concrete such as steel fiber and glass fiber. Wood material possesses its own peculiar properties such as porosity, absorptivity, as well as a large amount of active groups such as covalent hydroxyl and carboxylic groups which exist on its surface.^{10–14} Therefore, information obtained from the observation of interfacial phenomena between wood and cement is considered beneficial for a better understanding in improving the mechanical properties of WCM.

In this study, in order to obtain information about the morphology, element distribution, and composition of hydration products at the wood–cement interfacial zone, which is influenced by various mixture compositions, scanning electron microscopy with energy dispersive X-ray spectroscopy (SEM-EDS) analysis was used as an aid in observing the microstructure and identifying the elemental composition of samples. In addition, X-ray diffraction (XRD) analysis was performed in parallel, to identify the hydration products and unhydrated cement clinkers in the different mixtures.

The main objectives of the current study were to: (1) investigate the Ca/Si ratios at the wood–cement interfacial zone in different mixtures, (2) make observations and comparisons of elemental compositions of hydration products in the different microregions such as the tracheid lumen and cement paste, and (3) investigate the morphology and elemental compositions of hydration products developed on the wood surfaces in the different mixtures.

Materials and methods

Materials

Weathered wood waste removed from service: sugi wood (*Cryptomeria japonica* D. Don), collected at construction sites, was used in this study. The wood waste with dimensions of 900 mm (L), 150 mm (W), and 25 mm (T) was initially soaked in water until a moisture content (MC) of 150%–200% was reached, and was then treated with the WVEP in a specially designed apparatus under the explosion conditions of temperature: 300°C, pressure: 2.5 MPa, and time: 4.0 min. Owing to the sudden decompression and water-vapor expansion (known as explosion), the wood waste was destructured and separated into wood fiber strand (WFS) with the irregular dimensions of about 100–250 mm in length and 1–4 mm in diameter.^{6,7} Unexploded wood waste with dimensions of 900 mm (L), 150 mm (W), and 25 mm (T) (sugi, water-soaked) was also used for comparison with the exploded WFS.

The commercial ordinary Portland cement (OPC) used in preparing WCM throughout this investigation was supplied by Taiheiyo Cement Co. Ltd. The chemical composition (wt %) of the cement is summarized in Table 1. Magnesium chloride (MgCl₂) was chosen as a suitable accelerator for cement hydration to enhance the compatibility between exploded WFS and cement based on the results described in earlier reports.^{8,9}

Sample preparation of wood–cement mixture

The exploded WFS and unexploded sugi wood were reduced to short fiber strand and wood strand (WS), respectively, with approximate dimensions of about 20 mm in length and 2–3 mm in diameter. All samples were prepared in a mixture of cement (200 g), wood (15 g, based on oven-dry weight), chemical additive (8 g), and distilled water (100 ml).

The hand-mixed sample was placed into a cylinder mold that was 8 cm in height, and 5.6 cm in diameter. After curing

Table 1. The main chemical composition of the ordinary Portland cement (OPC) employed in this study

	Composition	OPC (wt %)
Oxides		
Silicon dioxide	SiO ₂	20.68
Aluminum oxide	Al ₂ O ₃	5.06
Ferric oxide	Fe ₂ O ₃	2.87
Calcium oxide	CaO	64.64
Magnesium oxide	MgO	1.19
Sulphur oxide	SO ₃	2.03
Sodium oxide	Na ₂ O	0.33
Potassium oxide	K ₂ O	0.42
Compounds		
Tricalcium silicate	3CaO · SiO ₂ (C ₃ S)	53
Dicalcium silicate	2CaO · SiO ₂ (C ₂ S)	21
Tricalcium aluminate	3CaO · Al ₂ O ₃ (C ₃ A)	9
Tetracalcium aluminoferrite	4CaO · Al ₂ O ₃ · Fe ₂ O ₃ (C ₄ AF)	9

for 24 h, the molded sample was carefully removed from the cylinder mold, and then cured for 28 days at ambient temperature of 20°–23°C. In addition, a sample of neat OPC was used as a reference corresponding to its mixture. Three replications of each sample were conducted in this study.

Sample preparation for scanning electron microscopy with energy-dispersive X-ray spectroscopy (SEM-EDS) and X-ray diffraction (XRD) analyses

Three mixtures with the different compositions: OPC + unexploded WS, OPC + exploded WFS, and OPC + exploded WFS + MgCl₂ (4%) were prepared. The samples that were subjected to SEM-EDS and XRD analyses were taken from the fractured parts of the cured mixtures after crushing. To obtain a significant and distinct sample surface including the interface between wood and cement, the short exploded WFS and unexploded WS, were used directly in the mixtures.

The fractured parts of the mixtures were initially treated with a subcarbonizing process using an oven under the treatment conditions of temperature: 200°C, time: 60 min, gas flow: nitrogen. Because the wood tissue contained in the mixture became weak and brittle after treatment, the fractured parts could be easily broken to obtain a sample with a smooth and flat observation surface suitable for SEM-EDS analysis. In addition, to observe the morphological features of hydration products formed at the interface after the removal of wood tissue, an attempt was to treat the fractured parts of the mixture with a temperature of 800°C for 30 min. Using photoglue (polyvinyl acetate), the treated sample was mounted on one end of a piece of copper tape, and the other end of the tape was adhered to a SEM sample stub. The orientation and angle of the sample surface for observation could be adjusted by bending the copper tape. A conductive paint was applied from the sample to the stub to ensure good electrical contact, and then the sample was dried in a low-temperature (50°C) oven for 4 h to allow glue hardening. Finally, the sample was coated with Pt–Pd (80:20) in an ion-sputter coater (Jeol JFC-1100) prior to SEM-EDS analysis.^{14,15}

The microstructural characteristics of the wood–cement interfacial zone influenced by the different mixture compositions were examined with a Jeol JSM–840 SEM coupled with a Jeol JED–2110 EDS analyzer. The SEM observation was conducted at an accelerating voltage of 5 keV, and EDS analysis at an accelerating voltage of 20 keV for spectrum analysis and element mapping. In addition, to identify the different hydration products, powder XRD analysis was performed in parallel, using Cu–K α radiation (35 kV and 30 mA) on a Jeol JDX-8200 X-ray diffractometer. The XRD scanning was run with 2θ ranged between 10° and 60° in steps of 0.02°.

Calculation and data analysis

The data collected using EDS spectrum analysis, were expressed as mean \pm standard deviation (SD). A multiple

comparison among sample population means was performed using the analysis of variance (ANOVA) to determine whether significant differences existed between sample population means at a 5% significance level. An associated probability (*P*-value) less than 5% was considered significant.¹⁶

Results and discussion

Observation and comparison of Ca/Si ratio at the interfacial zone of WCM with different compositions

The microstructural characteristics of the interfacial zone between wood and cement are considered to play an important role in obtaining good wood–cement adhesion, because they are directly associated with the wood–cement bond quality, and thus influence the mechanical properties and the durability of WCM.

In an earlier study, to understand the correlations between the hydration characteristics and mechanical performance, compression strength tests were conducted in parallel to hydration tests of exploded WFS–cement mixtures of different compositions. As a supplementary test, a primary analysis of element distributions at the wood–cement interfacial zone of different mixtures was performed using SEM-EDS analysis. The results indicated that the distributions of Ca and Si at the wood–cement interfacial zone were significantly different from those in the other parts of the mixture, and were noticeably influenced by the mixture compositions. In the case of the mixtures with unexploded WS present, or exploded WFS added with MgCl₂ (4%), the increase in the concentrations of Ca and Si toward the wood surface was detected at the wood–cement interface. However, similar increases in concentrations of these elements were not found in the mixture with exploded WFS added alone.⁹

The SEM micrographs of Fig. 1 show the general appearances of the wood–cement interfacial zones from the fractured surfaces of three mixtures: OPC + unexploded WS, OPC + exploded WFS, and OPC + exploded WFS + MgCl₂ (4%). Figure 2 shows the distribution profiles of Ca/Si ratios, based on EDS spectrum analysis, in the cement paste as a function of the distance from the wood–cement interfaces (shown in Fig. 1). Relatively high Ca/Si ratios were found at the interface in the mixtures with unexploded WS or exploded WFS with added MgCl₂ (4%). The increase in Ca/Si ratios of these mixtures was detected in their cement pastes at distances of 0–40 μ m from the interface. For the mixtures with unexploded WS or exploded WFS with MgCl₂, the Ca/Si ratios reached maximum values of about 4.9 and 4.7, respectively. However, an approximately unchanged Ca/Si ratio of about 3.5 was observed throughout the cement paste for the mixture containing only exploded WFS. This result showed that although it was consistent with results obtained in a previous study⁹ which showed that the higher concentrations of Ca and Si were observed at the wood surface, the extent of increases in concentrations of

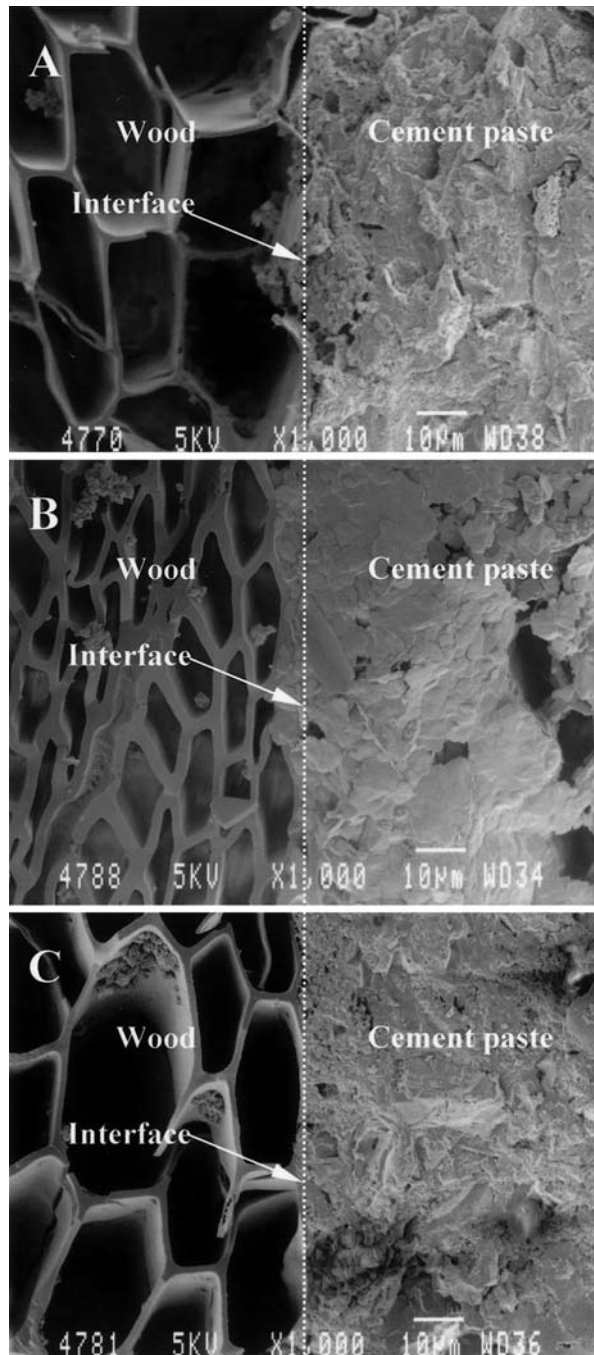


Fig. 1A–C. Scanning electron microscopy (SEM) micrographs of the microregions including wood–cement interfaces from the mixtures with different compositions. **A** Ordinary Portland cement (OPC) + unexploded wood strand (WS), **B** OPC + exploded wood fiber strand (WFS), **C** OPC + exploded WFS + MgCl_2 (4%). The fractured surfaces of the mixtures were treated with a subcarbonizing process for SEM-EDS analysis. Bars $10\mu\text{m}$

Ca and Si were significantly different. The increase in concentration of Ca was noticeably higher than that of Si, and this is attributed to the fact that Ca^{2+} ion has a higher mobility than Si^{4+} ion in cement solution. This would result in the different Ca/Si ratios at the wood–cement interface. In addition, the results obtained in this study imply that

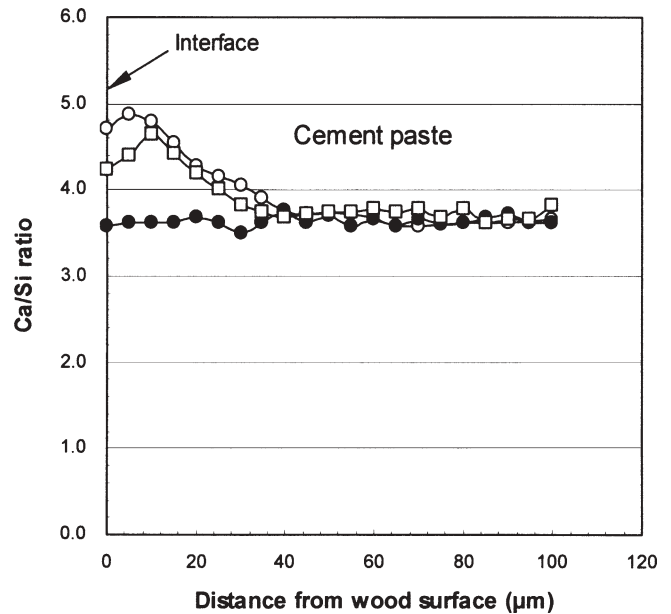


Fig. 2. Ca/Si ratio of cement paste as a function of the distance from wood–cement interface for the mixtures with different compositions. *Open circles*, OPC + unexploded WS; *closed circles*, OPC + exploded WFS; *squares*, OPC + exploded WFS + MgCl_2 (4%)

there was a gradient increase and accumulation of hydration products such as calcium hydroxide (CH) crystals and calcium silicate hydrates (CSH) close to the wood–cement interfaces, corresponding to an uninhibited or an accelerated wood–cement mixture, these hydration products lead to the formation of the relatively high bond strengths between wood and cement. The different Ca/Si ratios at the interfaces were considered as being an indicator of the development (retarded or accelerated) of cement hydration reactions corresponding to the different mixture compositions. The results were also consistent with those obtained in both hydration behavior tests and compression strength tests of the mixtures in an earlier study.^{8,9}

The increase in concentrations of Ca and Si at the wood–cement interfacial zone was more directly observed by EDS elemental dot maps. With a color scale, different colors were assigned for each concentration level of the elements mapped. For example, Fig. 3A,B shows typical images as acquired with Ca and Si dot maps, which were detected from a fractured surface including the exploded WFS–cement interface with added MgCl_2 (4%), shown in Fig. 1C. In the microregion close to the interface, concentrations of Ca and Si were higher than those in the rest of the cement paste.

In several previous investigations that dealt with the interfacial characteristics of cement mixtures reinforced with steel fiber or glass fiber, a three-phase model: fiber, interfacial zone, and cement paste was suggested to describe the microstructure of the mixture. The interfacial zone between cement and reinforcement materials was known to be the weakest zone relating to the strength performance due to its porosity.^{17–19} However this model was, seemingly, not able to explain the microstructure in the wood–cement interfa-

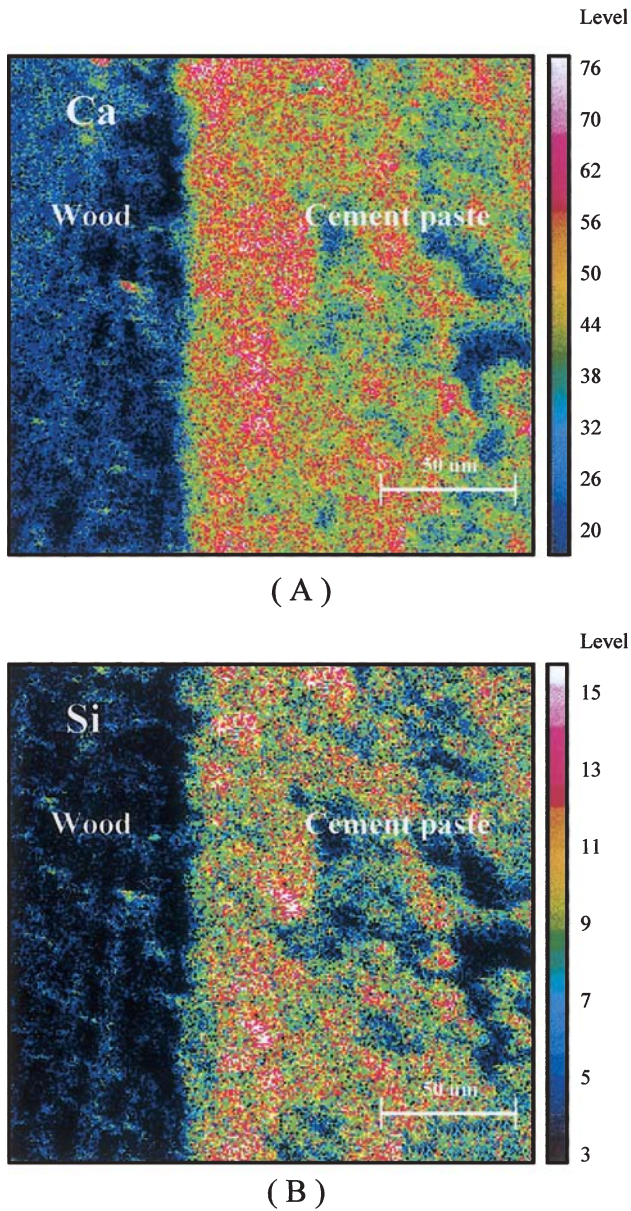


Fig. 3. Energy dispersive X-ray spectroscopy (EDS) dot maps of **A** Ca and **B** Si at the wood–cement interfacial zone of OPC + exploded WFS + MgCl_2 (4%). Bars $50\mu\text{m}$

cial zone. Unlike the reinforcement materials mentioned above which possess almost impenetrable surfaces when faced to cement paste, wood exhibits water absorptivity due to its porous and penetrable surface structure as well as its chemical composition.

The bond between wood and cement is physical or chemical in nature, or a combination of both. Some previous studies suggested that the mechanical interlocking (sometimes known as anchorage) which was brought about by the various crystals and hydration products developed on the wood surface during the cement hydration, play a significant role in the formation of bonding between wood and cement.^{20–22} At the initial stage of cement hydration, large amount of ions such as Ca^{2+} and Si^{4+} in cement clinker will

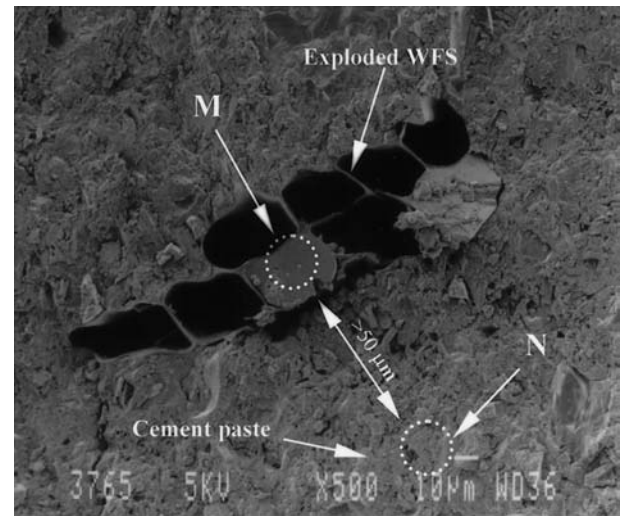


Fig. 4. SEM micrograph of tracheid lumen filled with hydration products near the wood–cement interface of OPC + exploded WFS + MgCl_2 (4%). *M*, hydration products in filled tracheid lumen; *N*, cement paste. Bar $10\mu\text{m}$

rapidly be dissolved into the cement solution. In fact, it should be emphasized that there is an ion diffusion process that occurs at the wood–cement interfacial zone, and thus when accompanied with solution flow, these ions move to the wood surface. Some ions will unavoidably permeate into the cell wall due to the existence of high concentration gradients of the ions at the penetrable wood surface. Thus, it is possible that the existence of these permeated ions in the cell wall results in mineralization of the cell wall, which promotes the affinity of the wood surface to cement. This mechanism may also contribute to the formation of interlocking between wood and cement by means of hydration products in addition to intermolecular forces.^{23–25}

Observation and comparison of elemental composition of hydration products deposited in tracheid lumen near the interface between wood and cement

Due to the ion diffusion process in cement solution which results in the migration of hydration products, it was usually observed that some hydration products were deposited in the tracheid lumen. These frequently formed cylindrical crystallized bodies near the interface between wood and cement (for example, see Fig. 4). To determine the elemental compositions of these hydration products in comparison with those in cement paste, EDS spectrum analysis was performed within the two microregions (*M* and *N*). The areas of interest are outlined by the circles located over the tracheid lumen and cement paste, as illustrated in Fig. 4. To determine the relatively steady elemental distributions in the cement paste (Fig. 2), micro region *N* was selected at a distance of more than $50\mu\text{m}$ from the wood–cement interface. The results of spectral analysis (as shown in Fig. 5) indicated that the elemental compositions of hydration products in the tracheid lumen and in cement paste were

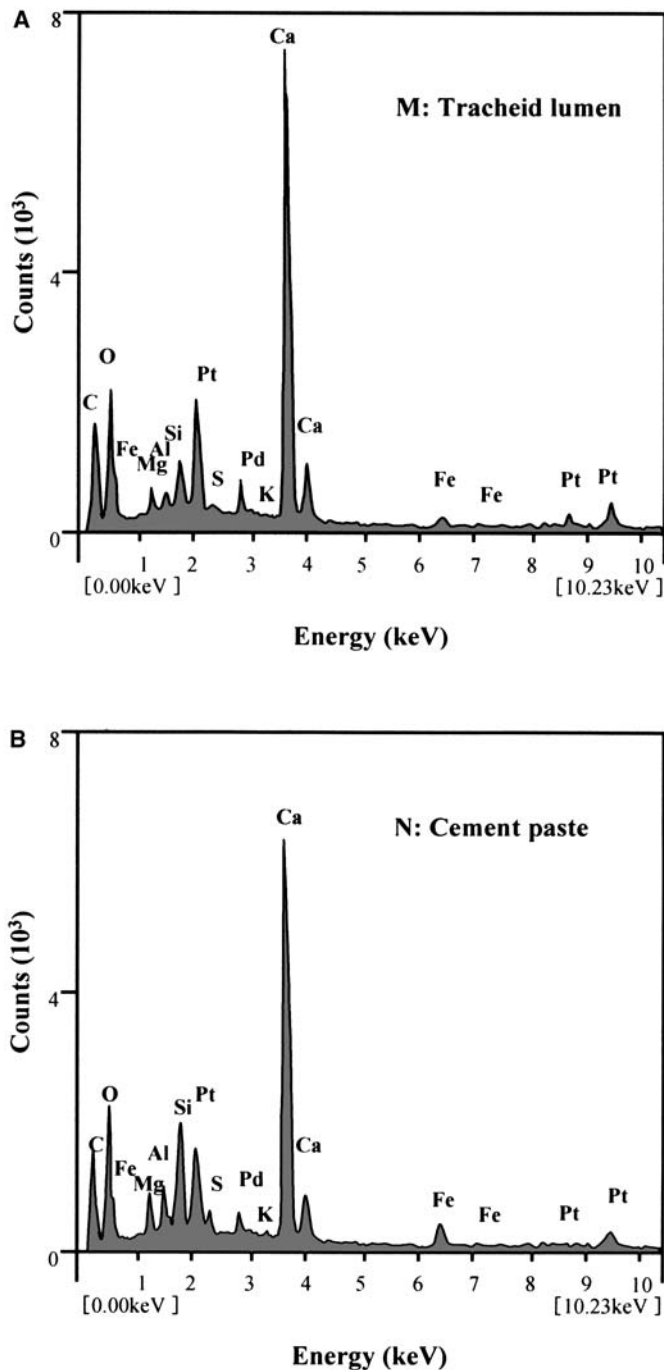


Fig. 5. EDS spectral profiles of hydration products filled in the **A** tracheid lumen (*M*) and **B** cement paste (*N*) as shown in Fig. 4

significantly different. In particular, higher amounts of Ca and smaller amounts of Si were found in tracheid lumen compared with those in cement paste. Spectral analysis were also conducted for the mixtures of different compositions. The elemental distributions (wt %) of Al, Fe, Mg, Ca, Si, and Ca/Si ratio mainly detected in both tracheid lumen and cement paste are summarized in Table 2. The results revealed that no significant differences in elemental compositions were found among the cement pastes of the three mixtures, and in neat hydrated OPC as well. However, com-

pared with cement paste, the elemental compositions of hydration products deposited in the tracheid lumen were statistically different. Very small amounts of Al, Fe, Mg, and Si were detected, and thus the hydration products in the tracheid lumen showed much higher Ca/Si ratios. These results implied that more CH crystals existed in the tracheid lumen. Moreover, the Ca/Si ratio of hydration products in the tracheid lumen was noticeably influenced by the mixture compositions. In particular, with the presence of exploded WFS in the mixture without added chemical additive, it was difficult to detect the existence of elements such as Al, Fe, and Mg. Due to the very low amount of Si, the highest Ca/Si ratio of the study (125.3) was observed. This phenomenon was not only attributed to the low mobility of the Si^{4+} ion, but also due to the presence of excess degraded polysaccharides in the extractives of exploded WFS. Thus, cement hydration in the mixture was severely inhibited, and even stopped at the initial stage, resulting in fewer Si^{4+} and other ions released into the cement solution.

Observation and comparison of morphological features and elemental compositions of hydration products developed on the surface of exploded WFS

The bond strength at the interface between wood and cement is considered to be critically influenced by the microstructure and morphology of hydration products that develop on the wood surface. However, the morphology of hydration products is highly sensitive to the mixture composition. A retarded cement hydration will lead to poor morphology of the hydration products, resulting in low bond strength, and consequently low mechanical performance of WCM.

Figure 6 shows the SEM micrographs obtained from observations of the fractured surfaces of exploded WFS–cement mixtures with and without added MgCl_2 (4%). As shown in the micrographs, differences in the microstructure and morphology of hydration products deposited on the surfaces of exploded WFS were evident. In Fig. 6A, apart from some small hexagonal plates of CH crystals, the conventionally due to the retarding effects of exploded WFS, observed morphology of typical hydration products such as CSH were not observed. However, the exploded WFS surface was covered with many unhydrated cement grains and short rod-like crystals. Thus, this loose and discontinuous microstructure adhering to the exploded WFS surface, seemingly, does not provide any contribution to strength development of the mixture. However, in the case of the mixture enhanced with added MgCl_2 (4%), as shown in Fig. 6B, there was a noticeable difference in the morphological features on the surface of exploded WFS in comparison to Fig. 6A. A network-like structure, which was attributed to the hydration product of CSH ($\text{CaO} \cdot \text{SiO}_2 \cdot \text{H}_2\text{O}$) in the honeycomb-like form of CSH (type II), adhered tightly to the exploded WFS surface.²⁶ This microstructure was believed to be beneficial for the formation of interlockings (anchorage) on the porous wood surface, which resulted in

Table 2. Energy dispersive X-ray spectroscopy (EDS) analysis of elemental compositions as detected at different microregions from the fractured surfaces of wood–cement mixtures

Mixture compositions	Chemical elements (wt %)					
	Al	Fe	Mg	Ca	Si	Ca/Si
Cement paste						
OPC	1.7 ^a (0.7) ^b	1.2 (0.0)	0.4 (0.1)	31.6 (6.8)	7.2 (0.2)	4.4 (0.9)
OPC + unexploded WS	1.1 (0.1)	1.1 (0.1)	0.5 (0.1)	28.5 (5.0)	6.2 (0.9)	4.6 (0.8)
OPC + exploded WFS	1.5 (0.4)	1.2 (0.4)	0.4 (0.3)	33.4 (3.4)	6.7 (1.4)	5.0 (1.1)
OPC + exploded WFS + MgCl ₂ (4%)	1.4 (0.3)	1.0 (0.2)	1.2 (0.3)	33.0 (2.9)	6.9 (1.0)	4.8 (1.2)
Tracheid lumen						
OPC	–	–	–	–	–	–
OPC + unexploded WS	0.1 (0.1)	0.2 (0.1)	0.0 (0.0)	35.8 (5.1)	1.3 (0.3)	27.5 (7.0)*
OPC + exploded WFS	0.0 (0.0)	0.1 (0.1)	0.0 (0.0)	25.1 (4.2)	0.2 (0.1)	125.3 (20.8)**
OPC + exploded WFS + MgCl ₂ (4%)	0.1 (0.1)	0.3 (0.1)	0.6 (0.3)	20.0 (6.2)	1.1 (0.5)	18.2 (6.1)*

OPC, ordinary Portland cement; WS, wood strand; WFS, wood fiber strand

*Means are significantly different at the 5% significance level

**Means are significantly different at the 1% significance level (based on the variance test analysis)

^aEach value is the average of 6 replications

^bData included in parentheses are standard deviation (SD)

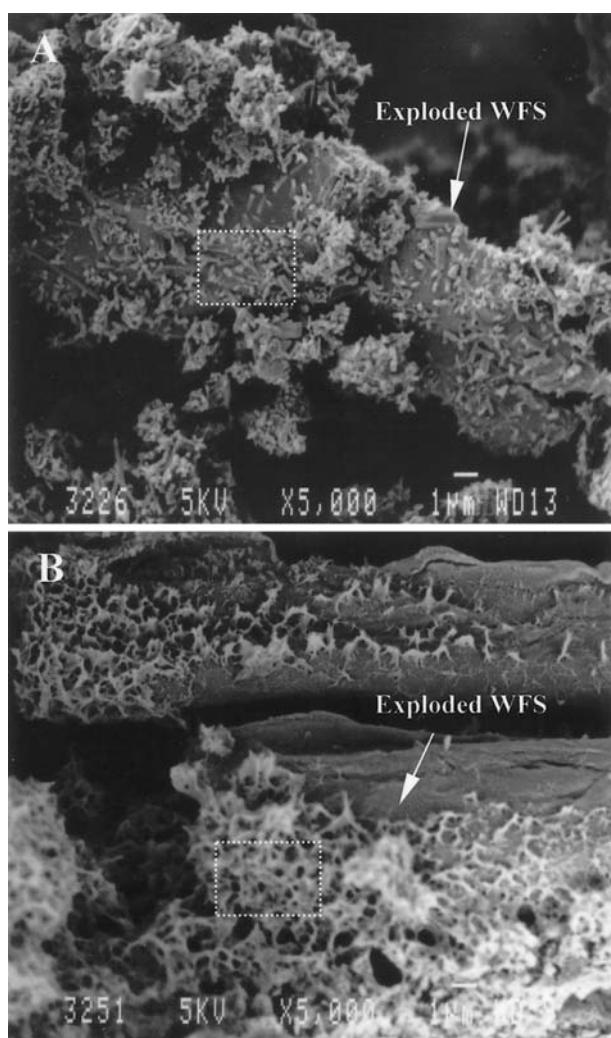


Fig. 6A,B. SEM micrographs of the hydration products on the surfaces of exploded WFS in different mixtures. **A** OPC + exploded WFS, **B** OPC + exploded WFS + MgCl₂ (4%). Bars 1 μm

the development of bond strength between the exploded WFS and cement.

In order to identify the elemental composition of hydration products that developed on the exploded WFS surfaces in the different mixtures, EDS spectral analysis was conducted over the microregions outlined by the squares shown in Fig. 6A,B. The results of spectral analysis are presented in Fig. 7. The two spectrum profiles demonstrated different patterns depending on the elemental compositions and distributions of hydration products deposited on the exploded WFS surfaces. Figure 7A shows an elemental spectrum in which relatively high amounts of S and Al, as well as Ca, were detected. Thus, the hydration products were quite consistent with the presence of ettringite (sometimes abbreviated to AFt, $3\text{CaO} \cdot \text{Al}_2\text{O}_3 \cdot 3\text{CaSO}_4 \cdot 32\text{H}_2\text{O}$), presumably formed at a very early hydration stage. As shown in Fig. 7B, a completely different spectrum profile of hydration products was obtained for the exploded WFS surface in the mixture with added MgCl₂, in which only high amounts of Ca and Si were detected. Essentially, a large portion of the hydration products contained in a well-hydrated OPC were CSH and CH crystals, or their complexes from hydration of $\text{C}_3\text{S}(3\text{CaO} \cdot \text{SiO}_2)$ and $\text{C}_2\text{S}(2\text{CaO} \cdot \text{SiO}_2)$ to develop a rigid microstructural network. Thus, these microstructures were thought to consist of CSH hydration products, or partially, CH crystals.

In addition, an attempt was made to treat the fractured surface of exploded WFS–cement mixtures at high temperature to obtain a surface of cement paste adjacent to the interface after removal of the wood. As presented in Fig. 8, a surface of cement paste with high porosity was clearly exposed. This porosity was attributed to the fact that a high Ca/Si ratio at the interface induced high amounts of CSH hydration products and CH crystals. Previous investigations have indicated that this porous microstructure of hydration products exists in the interfacial zone and plays an important role in determining the durability of the mixture.^{11,17}

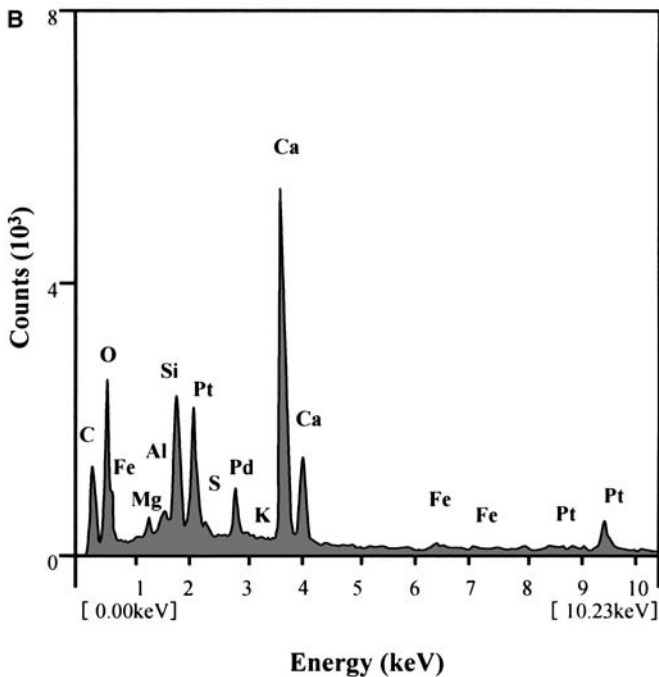
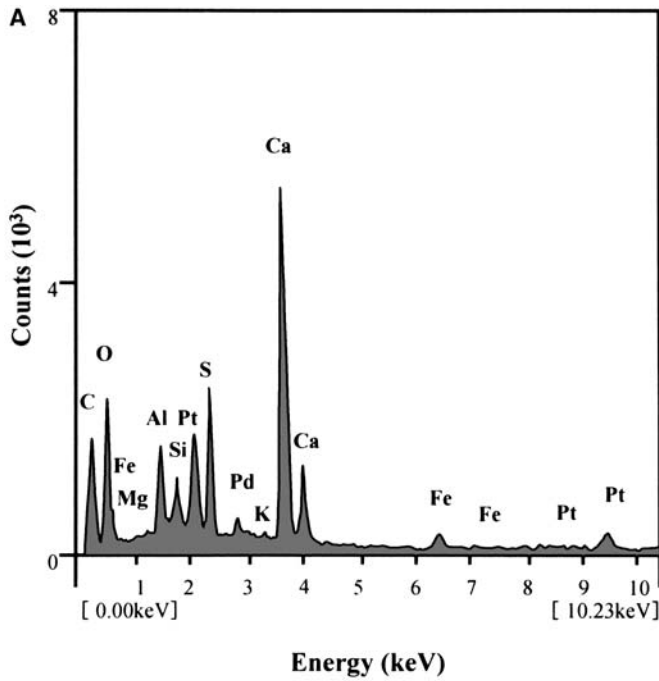


Fig. 7A,B. EDS spectral profiles of the hydration products on the surfaces of exploded WFS in different mixtures. **A** OPC + exploded WFS, **B** OPC + exploded WFS + $MgCl_2$ (4%)

Under close observation, a large amount of disk-shaped hydration products were found on the surface of the cement paste (as illustrated by arrowheads in Fig. 8). This material was formed in the bordered pit chambers on the longitudinal tracheid wall during the initial stage of cement hydration when the cement solution has a high fluidity. It is considered that this disk-shaped microstructure of hydra-

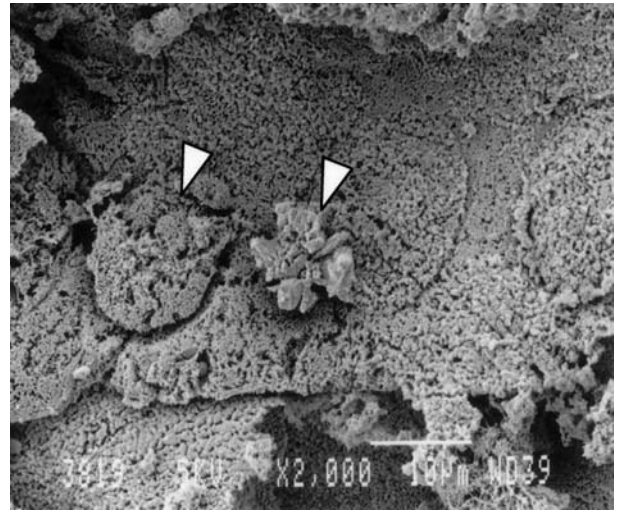


Fig. 8. SEM micrograph of the surface of cement paste after the removal of wood showing disc-shaped hydration products (arrowheads). The mixture of OPC + exploded WFS + $MgCl_2$ (4%) was treated at high temperature to remove wood from the fractured surface of the mixture. Bar $10\mu m$

tion products could provide a supplementary mechanical bond between exploded WFS and cement.

X-ray diffraction

In order to obtain more information about cement hydration in the mixtures with different compositions, X-ray diffraction (XRD) analysis was conducted on the three mixtures: OPC + unexploded WS (C), OPC + exploded WFS (D), and OPC + exploded WFS with $MgCl_2$ (4%) (E). Furthermore, the unhydrated neat OPC (A) and hydrated neat OPC (B) were used as reference materials. Samples B–E were cured for 28 days prior to analysis. The XRD spectral profiles of samples A–E are illustrated in Fig. 9.

In these spectral profiles, the main peaks were assigned to the unhydrated cement clinkers of C_3S ($3CaO \cdot SiO_2$) and C_2S ($2CaO \cdot SiO_2$), located at $d(\text{\AA}) = 3.022, 2.776, 2.764, 2.602, 2.185, 1.771, \text{ and } 1.632$ ($2\theta = 29.2^\circ, 32.3^\circ, 32.7^\circ, 34.5^\circ, 41.1^\circ, 51.1^\circ, \text{ and } 56.4^\circ$), and the major hydration product of CH located at $d(\text{\AA}) = 4.900$ ($2\theta = 17.8^\circ$). These peaks were used to evaluate the influences of the different mixture compositions on cement hydration in this study. The peaks denoted by C_3S/C_2S at $2\theta = 32.3^\circ, 32.7^\circ, \text{ and } 56.4^\circ$, in Fig. 9 are the overlapped peaks of C_3S and C_2S .^{26–28}

It was clearly evident that in the mixture of OPC + exploded WFS (sample D), no peak corresponding to the CH crystal at $2\theta = 17.8^\circ$ was observed. However, the peaks at $2\theta = 29.2^\circ, 32.3^\circ, 32.7^\circ, 34.5^\circ, 41.1^\circ, 51.1^\circ, \text{ and } 56.4^\circ$, which represent the unhydrated cement clinkers, showed strong intensities and no significant differences in pattern in comparison with the unhydrated neat OPC (sample A). Therefore, these findings indicated that cement hydration was completely inhibited, due to the presence of degraded

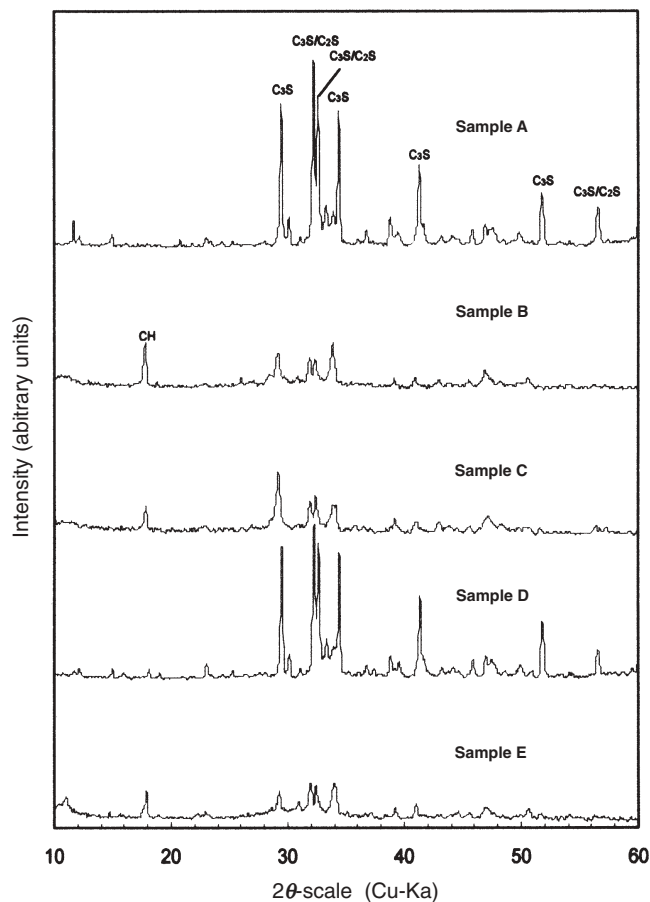


Fig. 9. Comparison of X-ray diffraction (XRD) spectra of mixtures with the different compositions. *Sample A*, unhydrated neat OPC; *sample B*, hydrated neat OPC; *sample C*, OPC + unexploded WS; *sample D*, OPC + exploded WFS; *sample E*, OPC + exploded WFS + MgCl_2 (4%); CH, $\text{Ca}(\text{OH})_2$; C_3S , $3\text{CaO}\cdot\text{SiO}_2$; C_2S , $2\text{CaO}\cdot\text{SiO}_2$

polysaccharides from exploded WFS. It was also observed that in comparison with the mixtures of unexploded WS (sample C), high-temperature and high-pressure treatment by WVEP revealed a significant negative effect on mixtures of exploded WFS and OPC.

However, with addition of MgCl_2 (4%), the compatibility between the exploded WFS and OPC (sample E) was greatly enhanced. A noticeable improvement in cement hydration was observed with the presence of the peak corresponding to the CH crystal at $2\theta = 17.8^\circ$, and the decreased, or absent peaks corresponding to unhydrated cement clinker at $2\theta = 29.2^\circ, 32.3^\circ, 32.7^\circ, 34.5^\circ, 41.1^\circ, 51.1^\circ$, and 56.4° . This mixture demonstrated a similar XRD pattern in comparison with the hydrated neat OPC (sample B), although an observable difference was that the intensity of the CH peak appeared slightly lower than that in the spectrum of hydrated neat OPC. The results obtained in XRD analysis were consistent with the results described in SEM-EDS analysis above.

Conclusions

Based on the combination of SEM observations and EDS analysis, the results obtained in this study are considered to agree well with the previous results that dealt with the evaluations of hydration behaviors and strength performances of exploded WFS–cement mixture. The following conclusions are made:

1. The Ca/Si ratio at the interface between wood and cement was significantly influenced by mixture compositions. The elevated Ca/Si ratio that was higher than that in the bulk of the cement paste was detected at the interface of mixtures with unexploded WS or exploded WFS with added MgCl_2 (4%). The local increase of Ca/Si ratios at interfaces implied that the interface zones accumulated more hydration products such as CH crystals, which were beneficial to the formation of interlocking between wood and cement, and resulted in better bond strength and higher mechanical strength.
2. EDS spectral analysis of elemental composition, performed both at the tracheid lumen and in the cement paste, revealed that the hydration products deposited in the tracheid lumen close to the wood–cement interface were detected with much higher Ca/Si ratios compared with those in cement paste. It indicated a higher accumulation of CH crystals in the tracheid lumen, probably due to the existence of the increased concentration gradient of Ca^{2+} ion at the interface.
3. SEM-EDS analysis of the hydration products that developed on the exploded WFS surfaces showed that there were clear differences in their morphological features and elemental compositions, which directly affect the bond strength between exploded WFS and cement as well as the mechanical strength of mixtures.
4. XRD analysis showed that the mixture with added exploded WFS demonstrated a spectral profile similar to that of unhydrated neat OPC, and no peaks for CH crystals were found. With the addition of MgCl_2 , the exploded WFS–cement mixture showed a spectral profile with CH peaks and decreased peaks corresponding to the unhydrated cement clinker.

Acknowledgments The authors are very grateful to Dr. Y. Tomimura and Dr. H. Abe, who are researchers at the Forestry and Forest Products Research Institute (FFPRI), Tsukuba, Japan, for their assistance in this study. We also thank the Taiheiyō Cement Corporation, Japan, for providing the data on cement composition.

References

1. Moslemi AA (1988) Inorganically bonded wood composites. *Chemtech* 18:504–510
2. Miller DP, Moslemi AA (1991) Wood-cement composites: effect of model compounds on hydration characteristics and tensile strength. *Wood Fiber Sci* 23:472–482
3. Yasuda S, Iwase Y, Seguchi Y, Takemura T, Matsushita Y (1992) Manufacture of wood cement boards V. Cement-hardening inhibitory components of sugi heartwood and behavior of catechol as a

- simple inhibitor model with vicinal phenolic hydroxyl groups in cement paste (in Japanese). *Mokuzai Gakkaishi* 38:52–58
4. Imai T, Suzuki M, Aoyama K, Kawasaki Y, Yasuda S (1995) Manufacture of wood cement boards VI. Cement hardening inhibitory compound of beech (*Fagus crenata* blume) (in Japanese). *Mokuzai Gakkaishi* 41:44–50
 5. Young JF (1972) A review of the mechanisms of set-retardation in portland cement pastes containing organic admixtures. *Cement Concrete Res* 2:415–433
 6. Fujii T (2000) Explosively-split fragments obtained by water-vapor explosion of wooden source materials, wooden material containing such fragments as its aggregate, their manufacturing methods and machines. European Patent No.1033212 A1
 7. Hiramatsu Y, Miyatake A, Fujii T, Wei YM, Tomita B (2001) Wood elements obtained by water vapor explosion of wood materials. Proceedings of the Symposium on Utilization of Agricultural and Forest Residues, Nanjing, China, pp 152–158
 8. Wei YM, Tomita B, Hiramatsu Y, Miyatake A, Fujii T (2002) Study of hydration behaviors of wood–cement mixtures: the compatibility of cement mixed with wood fiber strand obtained in the water-vapor explosion process. *J Wood Sci* 48:365–373
 9. Wei YM, Tomita B, Hiramatsu Y, Miyatake A, Fujii T, Fujii T, Yoshinaga S (2003) Hydration behavior and compressive strength of cement mixed with exploded wood fiber strand obtained by the water-vapor explosion process. *J Wood Sci* 49:317–326
 10. Bentur A, Akers ASA (1989) The microstructure and ageing of cellulose fiber reinforced cement composites cured in a normal environment. *Int J Cement Comp Lightweight Concrete* 11:99–109
 11. Holmer S Jr, Vahan A (1999) Transition zone studies of vegetable fiber-cement paste composites. *Cement Concrete Comp* 21:49–57
 12. Swamy RN (1988) Natural fibre reinforced cement and concrete. In: *Concrete technology and design*, vol 5. Blackie, London, pp 15–46
 13. Fujii T, Miyatake A, Fujii T (1998) Manufacturing and property of cement-strand slab (CSS) (II): microscopic observation on interface of sugi strand and cement (in Japanese). Proceedings of the 48th Annual Meeting of the Japan Wood Research Society, Shizuoka, Japan, p 273
 14. Fujii T, Miyatake A (2003) SEM-EDXA study on the interface between wood and cement in cement strand slab. *Bulletin of the Forestry and Forest Products Research Institute*, 2:93–109
 15. Fujii T (2000) Scanning electron microscope (in Japanese). Edited by Kanto branch of the Japanese Society of Electron Microscopy. Kyoritsu, Tokyo, pp 397–402
 16. Lyman O (1977) An introduction to statistical methods and data analysis. Belmont Duxbury, North Scituate, pp 354–365
 17. Olliver JP, Maso JC, Bourdette B (1995) Interfacial transition zone in concrete. *Adv Cem Based Mater* 2:30–38
 18. Neubauer CM, Jennings HM, Garboczi EJ (1996) A three-phase model of the elastic and shrinkage properties of mortar. *Adv Cem Based Mater* 4:6–20
 19. Wasserman R, Bentur A (1996) Interfacial interactions in lightweight aggregate concretes and their influence on the concrete strength. *Cement Concrete Comp* 18:67–76
 20. Ahn WY, Moslemi AA (1980) SEM examination of wood–portland cement bonds. *Wood Sci* 13:77–829
 21. Kayahara M, Tajika K, Nakagawa H (1979) Strength increase of wood–cement composites (in Japanese). *Mokuzai Gakkaishi* 25:552–557
 22. Coutts RSP, Kightly P (1984) Bonding in wood fibre–cement composites. *J Mater Sci* 19:3355–3359
 23. Chatterji S (1998) Colloid electrochemistry of saturated cement paste and some properties of cement based materials. *Adv Cem Based Mater* 7:102–108
 24. Saka S, Sasaki M, Tanahashi M (1992) Wood–inorganic composites prepared by sol-gel processing I. Wood–inorganic composites (in Japanese). *Mokuzai Gakkaishi* 38:1043–1049
 25. Filho RDT, Scrivener K, England GL, Ghavami K (2000) Durability of alkali-sensitive sisal and coconut fibres in cement mortar composites. *Cement Concrete Comp* 22:127–143
 26. Nagadomi W, Kuroki Y, Eusebio DA, Ma LF, Kawai S, Sasaki H (1996) Rapid curing of cement-bonded particleboards II. Curing mechanism of cement with sodium hydrogen carbonate during steam injection pressing (in Japanese). *Mokuzai Gakkaishi* 42:659–667
 27. Tachi M, Nagadomi W, Tange J, Yasuda S, Terashima N (1987) Manufacture of wood–cement boards I. Influence on cement-hardening inhibition by the extractives from western redcedar heartwood (in Japanese). *Mokuzai Gakkaishi* 33:879–883
 28. Lea FM (1970) *The chemistry of cement and concrete*, 3rd edn. Bell and Bain, Glasgow, pp 171–337